Design and Experiment of a Prescribed-Time Trajectory Tracking Controller for a 7-DOF Robot Manipulator

Alexander Bertino
Dynamic Systems and Control Laboratory,
Department of Mechanical Engineering,
San Diego State University,
San Diego, CA 92182
e-mail: abertino6245@sdsu.edu

Peiman Naseradinmousavi
Dynamic Systems and Control Laboratory,
Department of Mechanical Engineering,
San Diego State University,
San Diego, CA 92182
e-mail: pnaseradinmousavi@sdsu.edu

Miroslav Krstic
Department of Mechanical and
Aerospace Engineering,
University of California, San Diego,
San Diego, CA 92093
e-mail: krstic@ucsd.edu

We present an analytical design and experimental verification of trajectory tracking control of a 7-DOF robot manipulator, which achieves convergence of all tracking errors to the origin within a finite terminal time, also referred to as the "settling time." A key feature of this control strategy is that the settling time is explicitly assigned by the control designer to a value desired, or "prescribed" by the user and that the settling time is independent of the initial conditions and of the reference signal. In order to achieve this beneficial property with the controller, a scaling of the state by a function of time that grows unbounded toward the terminal time is employed. Through Lyapunov analysis, we first demonstrate that the proposed controller achieves regulation of all tracking errors within the prescribed time as well as the uniform boundedness of the joint torques, even in the presence of a matched, nonvanishing disturbance. Then, through both simulation and experiment, we demonstrate that the proposed controller is capable of converging to the desired trajectory within the prescribed time, despite large distance between the initial conditions and the reference trajectory, i.e., in spite of large initial tracking errors, and in spite of a sinusoidal disturbance being applied in each joint.
[DOI: 10.1115/1.4055023]

1 Introduction

In many applications where robot manipulators are utilized, the convergence time of the underlying controller plays a crucial role. In many tasks, there are strict requirements on the maximum duration of convergence, and thus a failure to achieve convergence by the required time could lead to the inability of the robot manipulator to perform its task. Convergence time also plays a role in the planning and reliability of robot manipulators. For example, if an accurate estimate of the convergence time is known for a certain task, an accurate and reliable estimate of the productivity of the robot manipulator can be made. Expanding on this point, when multiple robot manipulators are used cooperatively, such as in an assembly line in industrial applications, having reliable estimates of the completion time of each individual task is crucial in order to effectively plan the operation of each manipulator. A considerable amount of research has been devoted toward the development of control methods for robot manipulators which are capable of guaranteeing an upper bound on the convergence time (potentially dependent on initial conditions), achieving convergence to zero within a finite period of time.

The literature on finite-time convergence methods concerning robot manipulators can be broadly organized into three distinct categories: the finite-time methods [1–5], the fixed-time methods [6–12], and the prescribed-time methods [13–25].

Finite-time methods are characterized by a finite convergence time that is bounded by the norm of the initial condition, as well as a function of the controller parameters. While these methods are useful in order to obtain more consistent convergence results, obtaining a specific desired convergence time requires determining the maximum initial conditions of the task to be completed, then tuning the controller parameters based on this value. Thus, in order to complete a larger set of tasks, with different initial conditions and maximum allowable operation times, separate controller parameters must be determined for each task.

Fixed-time methods are characterized by a finite convergence time that is bounded by a function of the controller parameters which is independent of the initial conditions. Thus, the process for tuning the controller parameters for a specific task is considerably simplified, as one no longer needs to consider the maximum expected initial conditions of the task, only the maximum required completion time. However, it is important to note that this upper bound of the convergence time is typically conservative, and thus the robot manipulator will usually complete the task well before the required completion time is exceeded. Additionally, depending on the implementation of the fixed-time controller, the upper bound of the finite convergence time may not be able to be arbitrarily set, meaning that certain maximum completion times may be too stringent for the controller to effectively handle.

Prescribed-time methods are characterized by a finite convergence time that is explicitly prescribed as a controller parameter. This desirable property of prescribed-time methods enables the same set of controller parameters to be utilized for a wide variety of tasks with different required completion times. Due to this desirable property, the development of prescribed-time methods has become an active research topic in recent years.

The first design of a prescribed-time stabilizing (and disturbance rejecting) controller was introduced by Song et al. [13], who employed a scaling of the state of a normal-form nonlinear system by a function of time that grows unbounded toward the terminal time. By stabilizing the system in the scaled representation, regulation in prescribed finite time is achieved for the original state, along with a smooth, uniformly bounded control input and the rejection of a matched nonvanishing disturbance. Another important class of prescribed-time controllers for robot manipulators, introduced by Becerra et al. [15] and improved upon by Obregón-Flores et al. [16], utilizes time base generators, which are state trajectories designed such that the system state smoothly converges to zero at the prescribed terminal time. A key feature, and arguably a disadvantage, of this control method, is the explicit use of the initial conditions in the controller structure as a feed forward term, along with a sliding-mode control scheme to correct for a uniformly bounded matched uncertainty. Notably, this scheme exhibits prescribed-time convergence in the ideal case of no matched uncertainty, and finite-time convergence when

Contributed by the Dynamic Systems Division of ASME for publication in the Journal of Dynamic Systems, Measurement, and Control. Manuscript received October 31, 2021; final manuscript received July 13, 2022; published online August 8, 2022. Assoc. Editor: Koushil Sreenath.

uncertainties are present. In a separate approach, Cao et al. [20] utilize a scaling system transformation technique to transform the Euler–Lagrange system considered into a new set of variables, in which the boundedness of the variables ensures that both partial and full state constraints will not be violated. In addition, this transformation also ensures that for any time greater than the prescribed convergence time, the remaining tracking errors will be less than a prescribed value. This approach is notable in that the scaling transformation utilized does not approach infinity as the terminal time is approached, and thus numerical difficulties caused by an unbounded gain are avoided in this method. However, a potential drawback to using this method is that the controller does not allow for separate control gains for each joint, meaning that aggressive torques are likely applied to certain joints of the robot manipulator when there is a large difference in inertia between joints, which is typically the case for high-DOF robot manipulators. In another approach, Garg and Panagou [12] utilize the concept of robust fixed-time control Lyapunov functions as well as control barrier functions to provide a framework for ensuring robustness to disturbances with fixed-time convergence to a user-defined goal set, along with ensuring the system state remains in a user-specified safe set throughout the operation.

In this effort, we reformulate the prescribed-time controller initially developed by Song et al. [13] in order to handle the case of trajectory tracking with a robot manipulator. This formulation yields convergence of the tracking errors to the origin within the prescribed terminal time, even in the presence of model uncertainties and a nonvanishing matched disturbance. Furthermore, in order to address the practical issues that can arise when employing an unbounded scaling of the state, due to factors such as measurement noise, numerical issues when applying a large scaling to small errors, and a finite controller frequency, we employ a gain-clipping strategy in order to limit the scaling of the state to a sufficiently high value. Through the experimental verification of this prescribed-time control strategy with gain clipping on Baxter, a 7-DOF redundant robot manipulator, we demonstrate convergence of the tracking errors to a small neighborhood of zero by the prescribed terminal time, despite a significant initial angular position tracking error of 20 deg on each joint, as well as a sinusoidal torque disturbance of $0.1 \sin 5t$ applied to each joint. Thus the prescribed-time control strategy studied here is both theoretically sound and effective in practice.

The organization of this paper is as follows. In Sec. 2, we present a brief overview of the dynamics of Baxter's right manipulator, as well as the conditions imposed on the design of the reference trajectory. In Sec. 3, we present the design of the prescribed-time trajectory-tracking controller. In Sec. 4, we demonstrate the prescribed-time regulation of the robot manipulator tracking errors through Lyapunov Analysis. In Sec. 5, we briefly discuss the practical implementation of the proposed control law. In Sec. 6, we present the simulation and experimental results of the proposed method implemented on Baxter's right manipulator, achieving convergence of the tracking errors to a small neighborhood of zero by the prescribed terminal time despite large initial tracking errors and a nonvanishing matched disturbance. Finally, in Sec. 7, we present the case that the proposed method is theoretically sound, straightforward to implement in a real system, and ultimately effective in practice.

Notations: In the following, we use the common definitions of class $\mathcal{K}$ and $\mathcal{KL}$ given in Ref. [26]. $|\cdot|$ refers to the Euclidean norm, the matrix norm is defined accordingly, for $M \in \mathcal{M}_\ell(\mathbb{R})(\ell \in \mathbb{N}^*)$, as $|M| = \sup_{|x|\leq 1} |Mx|$ and the spatial norm is defined as follows:

$$||f||_{[a,b]} = \sup_{t\in[a,b]} |f(t)|$$

2 Mathematical Modeling

The redundant manipulator, which is being studied here, has 7-DOF as shown in Fig. 1. The Baxter manipulator's

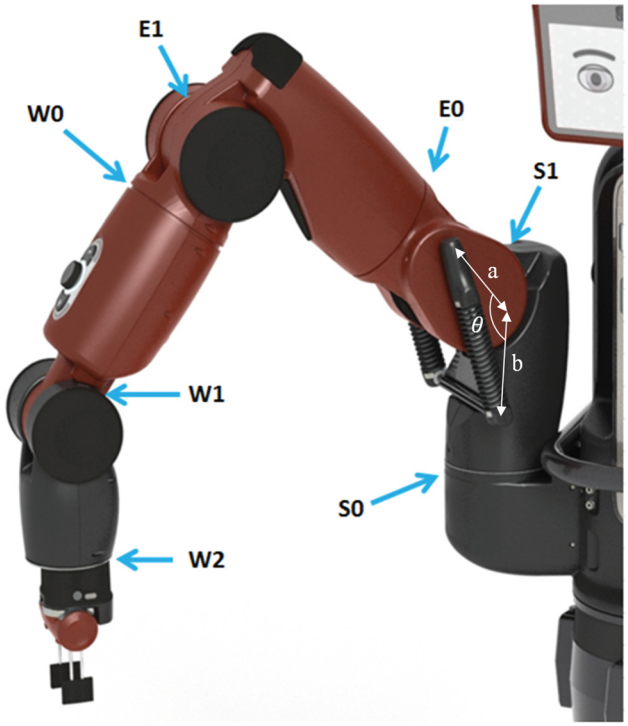

Fig. 1 The 7-DOF Baxter's arm at DSCL

Table 1 Baxter's Denavit–Hartenberg Parameters

Link	a_i	d_i	α_i	q_i
1	0.069	0.27035	$-\pi/2$	q_1
2	0	0	$\pi/2$	$q_2 + \pi/2$
3	0.069	0.36435	$-\pi/2$	q_3
4	0	0	$\pi/2$	q_4
5	0.010	0.37429	$-\pi/2$	q_5
6	0	0	$\pi/2$	q_6
7	0	0.3945	0	q_7

Denavit–Hartenberg parameters are shown in Table 1 provided by the manufacturer. The Euler–Lagrange formulation leads to a set of 7 coupled nonlinear second-order ordinary differential equations

$$M(q)\ddot{q} + C(q,\dot{q})\dot{q} + G(q) + F(\dot{q}) + D(t) = \tau \tag{1}$$

where, $q, \dot{q}, \ddot{q} \in \mathbb{R}^7$ are angles, angular velocities, and angular accelerations of joints, respectively, and $\tau \in \mathbb{R}^7$ indicates the vector of joints' driving torques. Also, $M(q) \in \mathbb{R}^{7\times7}$ is a symmetric mass-inertia matrix, $C(q,\dot{q}) \in \mathbb{R}^{7\times7}$ is a matrix of Coriolis coefficients, $G(q) \in \mathbb{R}^7$ is a vector of gravitational loading, $F(\dot{q}) \in \mathbb{R}^7$ represents a vector of frictional torques, and $D(t) \in \mathbb{R}^7$ is a vector of disturbance torques with an unknown bound applied to the system (Fig. 2).

Our verified coupled nonlinear dynamic model of the robot [27–38] is used as the basis of the prescribed-time approach. In order to formulate a controller that is robust to modeling uncertainty, the values of the mass matrix, gravity vector, and frictional torques derived from this dynamic model are treated as estimates, and are denoted as $\hat{M}(q), \hat{G}(q), \hat{F}(\dot{q})$, respectively. We make the following assumptions concerning the difference between our dynamic model and the true dynamics of Baxter:

ASSUMPTION 1. *The true and estimated values of the mass matrix, Coriolis matrix, gravity vector, frictional torques, and the disturbance torques satisfy the following inequalities*

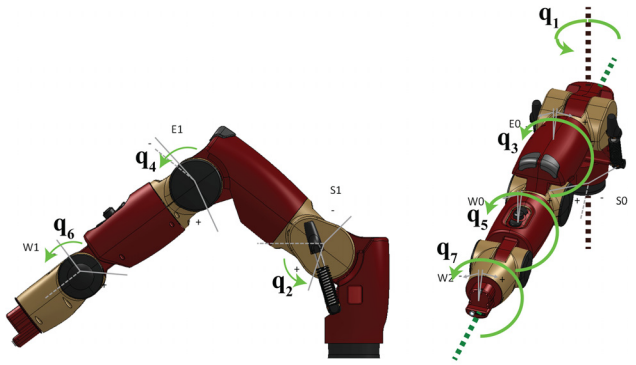

Fig. 2 The joints' configuration: (*a*) sagittal view and (*b*) top view

$$|M^{-1}(q)\hat{M}(q) - I| \leq c_1 \tag{2}$$

$$|M^{-1}(q)C(q,\dot{q})\dot{q}| \leq c_2|\dot{q}|^2 \tag{3}$$

$$|M^{-1}(q)(\hat{G}(q) - G(q))| \leq c_3 \tag{4}$$

$$|M^{-1}(q)(\hat{F}(\dot{q}) - F(\dot{q}))| \leq c_4|\dot{q}| \tag{5}$$

$$|M^{-1}(q)D(t)| \leq c_5|D(t)| \tag{6}$$

ASSUMPTION 2. *The true mass matrix $M(q)$, and the estimated mass matrix $\hat{M}(q)$ are symmetric and positive definite.*

Furthermore, we make the following assumption regarding the reference joint trajectories:

ASSUMPTION 3. *The desired joint trajectories are designed such that $q_r(t)$, $\dot{q}_r(t)$, and $\ddot{q}_r(t) \in \mathbb{R}^7$ exist and are uniformly bounded for all $t \in [0,T]$, where $T>0$ is the prescribed terminal time.*

3 Prescribed-Time Tracking for Robot Manipulators

We consider the following trajectory tracking system

$$\dot{E} = \begin{bmatrix} \dot{E}_1 \\ \dot{E}_2 \end{bmatrix} = \begin{bmatrix} E_2 \\ M^{-1}(\tau - C\dot{q} - G - F - D) - \ddot{q}_r \end{bmatrix} \tag{7}$$

$$E = \begin{bmatrix} \varepsilon \\ \dot{\varepsilon} \end{bmatrix} = \begin{bmatrix} E_1 \\ E_2 \end{bmatrix} = \begin{bmatrix} q - q_r \\ \dot{q} - \dot{q}_r \end{bmatrix} \tag{8}$$

where $E \in \mathbb{R}^{14}$ is the state error vector, and $\varepsilon \in \mathbb{R}^7$ is the vector of joint angular position tracking errors.

In order to regulate this system in prescribed-time, we first introduce the following monotonically increasing scaling function, as well as it's inverse

$$\mu_1(t) = \frac{T}{T-t}, \quad t \in [0,T) \tag{9}$$

$$\nu_1(t) = \frac{1}{\mu_1(t)} = \frac{T-t}{T}, \quad t \in [0,T) \tag{10}$$

where $T>0$ is the prescribed terminal time, with the properties $\mu_1(0)=1$, $\mu_1(T)=+\infty$, $\nu_1(0)=1$ and $\nu_1(T)=0$. To achieve prescribed-time regulation of the tracking errors, we introduce the following change of coordinates

$$w(t) = \mu(t)\varepsilon(t) \tag{11}$$

$$z(t) = \dot{w}(t) + \alpha w(t) \tag{12}$$

where

$$\mu(t) = \mu_1(t)^2 = \frac{1}{\nu_1^2} \tag{13}$$

and $\alpha > 0$. This change of coordinates results in the following forward and inverse scaling transforms

$$Z = \begin{bmatrix} w \\ z \end{bmatrix} = \mu \begin{bmatrix} I & 0 \\ \left(\alpha + \mu_1 \frac{2}{T}\right) I & I \end{bmatrix} E = P(\mu_1)E \tag{14}$$

$$E = \nu_1 \begin{bmatrix} \nu_1 I & 0 \\ \left(-\nu_1\alpha - \frac{2}{T}\right) I & \nu_1 I \end{bmatrix} Z = Q(\nu_1)Z \tag{15}$$

where $I \in \mathbb{R}_{7\times7}$ is the identity matrix, $P(\mu_1) \in \mathbb{R}^{7\times7}$ is the forward scaling transform, $Q(\nu_1) \in \mathbb{R}^{7\times7}$ is the inverse scaling transform, and $Z \in \mathbb{R}^{14}$ is the scaled state error vector. By taking the time derivative of (14) and substituting the inverse transformation (15), the dynamics of the scaled state error vector are obtained

$$\dot{w} = z - \alpha w \tag{16}$$

$$\dot{z} = \mu\left[\ddot{\varepsilon} - \left(\alpha^2\nu_1^2 + \alpha\nu_1\frac{4}{T} + \frac{2}{T^2}\right)w + \left(\nu_1\frac{4}{T} + \alpha\nu_1^2\right)z\right] \tag{17}$$

where

$$\ddot{\varepsilon} = M^{-1}(\tau - C\dot{q} - G - F - D) - \ddot{q}_r \tag{18}$$

Before presenting the design of the prescribed-time control law, it is first necessary to present several definitions concerning notions of stability within a finite prescribed interval of time.

DEFINITION 1 (FT-ISS [13]). *The system $\dot{x} = f(x,t,d)$ (of arbitrary dimensions of x and d) is said to be fixed-time input-to-state stable in time T (FT-ISS) if there exists a class $\mathcal{KL}$ function β and a class $\mathcal{K}$ function γ, such that, for all $t \in [0,T)$*

$$|x(t)| \leq \beta(|x_0|, \mu_1(t) - 1) + \gamma(||d||_{[0,t]}) \tag{19}$$

DEFINITION 2 (FT-ISS+C [13]). *The system $\dot{x} = f(x,t,d)$ (of arbitrary dimensions of x and d) is said to be fixed-time input-to-state stable in time T and convergent to zero (FT-ISS+C) if there exist class $\mathcal{KL}$ functions β and β_f, and a class $\mathcal{K}$ function γ, such that, for all $t \in [0,T)$*

$$|x(t)| \leq \beta_f(\beta(|x_0|, \mu_1(t) - 1) + \gamma(||d||_{[0,t]}), \mu_1(t) - 1) \tag{20}$$

As the function $\mu_1(t) - 1$ starts at zero and grows monotonically to infinity as $t \to T$, a system that is FT-ISS is also ISS, with the additional property that in the absence of a disturbance d, it is fixed-time globally asymptotically stable in time T. Additionally, a system that is FT-ISS+C is also FT-ISS, with the additional property that the state converges to zero even in the presence of a disturbance.

Now, we present the design of the prescribed-time control law.

THEOREM 1. *Under Assumptions 1–3, consider the system (7) with the controller*

$$\tau(t) = -\hat{M}(q)[(k + \theta + \eta\psi(\dot{q})^2)z(t) + \ddot{q}_r(t)] + \hat{G}(q) + \hat{F}(\dot{q}) \tag{21}$$

where

$$\psi(\dot{q}) = |\dot{q}|^2 + |\dot{q}| + 1 \tag{22}$$

If the controller gains are chosen such that $\rho, k, \eta > 0$

$$\rho k \alpha^2 > \frac{1}{4\lambda_M^2} \tag{23}$$

and

$$\theta \geq \frac{1}{\lambda_M}\left(\alpha + \frac{4}{T}\right) + \rho\left(\alpha^2 + \alpha\frac{4}{T} + \frac{2}{T^2}\right)^2 \tag{24}$$

where

$$\lambda_M = \min_{q\in[0,2\pi)} \lambda_{\min}\left(\frac{M^{-1}(q)\hat{M}(q) + \hat{M}(q)M^{-1}(q)}{2}\right) \tag{25}$$

then the closed-loop *system (7) with (21) is FT-ISS+C and the joint torques* τ *remain bounded over* $[0, T)$.

4 Lyapunov Analysis

For the purpose of the Lyapunov analysis, we propose the following Lyapunov function

$$V = \frac{1}{2}|z|^2 \tag{26}$$

Taking the derivative of this function yields

$$\begin{aligned}\dot{V} = \mu z^T \Big[& -M^{-1}\hat{M}\left(k + \theta + \eta\psi^2\right)z + \left(M^{-1}\hat{M} - I\right)\ddot{q}_r \\ & + M^{-1}\left(\hat{G} - G + \hat{F} - F - C\dot{q} - D\right) - \left(\alpha^2\nu_1^2 + \alpha\nu_1\frac{4}{T} + \frac{2}{T^2}\right)w \\ & + \left(\frac{4}{T}\nu_1 + \alpha\nu_1^2\right)z\Big]\end{aligned} \tag{27}$$

First, we seek to obtain an upper bound for the 1st term of $\dot{V}$. Utilizing the positive definite symmetric property of the mass matrices as stated in Assumption 2, we obtain the following inequality

$$z^T M^{-1}\hat{M}z = z^T\left(\frac{M^{-1}\hat{M} + \hat{M}M^{-1}}{2}\right)z \geq \lambda_M|z|^2 \tag{28}$$

where λ_M is first defined in (25).

Next, we examine the second and third terms of $\dot{V}$. Through the application of Assumptions 1 and 3, the following inequality can be obtained

$$\left(M^{-1}\hat{M} - I\right)\ddot{q}_r + M^{-1}\left(\hat{G} - G + \hat{F} - F - C\dot{q} - D\right) \leq \psi d \tag{29}$$

where

$$d(t) = \max\{c_1||\ddot{q}_r||_{[0,t]} + c_3 + c_5||D||_{[0,t]}, c_2, c_4\} \tag{30}$$

Applying (28) and (29) to (27), along with Young's inequality yields the following inequality

$$\begin{aligned}\dot{V} \leq & -\mu\lambda_M|z|^2\left(k + \theta + \eta\psi^2\right) + \mu\eta\lambda_M\psi^2|z|^2 \\ & + \frac{\mu}{4\eta\lambda_M}d^2 + \mu\rho\lambda_M|z|^2\left(\alpha^2\nu_1^2 + \alpha\nu_1\frac{4}{T} + \frac{2}{T^2}\right) \\ & + \frac{\mu}{4\rho\lambda_M}|w|^2 + \mu|z|^2\left(\frac{4}{T}\nu_1 + \alpha\nu_1^2\right)\end{aligned} \tag{31}$$

Through the application of (24), this inequality can be further reduced

$$\dot{V} \leq -2\mu\lambda_M kV + \frac{\mu}{4\eta\lambda_M}d^2 + \frac{\mu}{4\rho\lambda_M}|w|^2 \tag{32}$$

In order to proceed with the Lyapunov analysis, it is necessary to introduce a technical lemma from the work of Song et al. [13]

Lemma 1. *If a continuously differentiable function* $V : [0, T) \to [0, +\infty)$ *satisfies*

$$\dot{V}(t) \leq -2k\mu(t)V(t) + \frac{\mu(t)}{4\lambda}d(t)^2 \tag{33}$$

for positive constants k, λ, *where* $\mu(t)$ *is defined in (9), then*

$$V(t) \leq \xi(t)^{2k}V(0) + \frac{||d||^2_{[0,t]}}{8k\lambda}, \quad \forall t \in [0, T) \tag{34}$$

where ξ *is the monotonically decreasing function*

$$\xi(t) = e^{T(1-\mu_1(t))} \tag{35}$$

with the properties that $\xi(0) = 1$ *and* $\xi(T) = 0$.

Through the application of this lemma to (32), it can be seen that

$$|z(t)| \leq \xi(t)^{\lambda_M k}|z_0| + \frac{1}{2\lambda_M\sqrt{k}}\left(\frac{||w||_{[0,t]}}{\sqrt{\rho}} + \frac{||d||_{[0,t]}}{\sqrt{\eta}}\right) \tag{36}$$

and thus the z-system is FT-ISS with respect to the w-input with a gain of $\frac{1}{2\lambda_M\sqrt{k\rho}}$ and is also FT-ISS with respect to the d-input. In order to obtain the behavior of the w-system, one can rearrange (12) to obtain $\dot{w}(t) = -\alpha w(t) + z(t)$. From this point, it is straightforward to obtain a bound on w

$$|w(t)| \leq |w_0|e^{-\alpha t} + \frac{1}{\alpha}||z||_{[0,t]} \tag{37}$$

and thus the w-system is ISS with respect to the z-input with a gain of $\frac{1}{\alpha}$. Thus by the small-gain theorem, if condition (23) is satisfied, then the combined system Z is ISS with respect to d and thus there exist constants $\Gamma, \delta, \gamma > 0$ such that

$$|Z(t)| \leq \Gamma|Z_0|e^{-\delta t} + \gamma||d||_{[0,t]} \tag{38}$$

Through the substitution of the scaling transformation (14) into the right side of (38), followed by the substitution of the resulting inequality into the right side of the inverse scaling transformation (15), the following inequality is obtained

$$|E(t)| \leq \nu_1(t)[\breve{\Gamma}\,|E_0|e^{-\delta t} + \breve{\gamma}\,||d||_{[0,t]}] \tag{39}$$

where

$$\breve{\Gamma} = \Gamma|P(1)|\max_{\nu_1\in[0,1]}|Q(\nu_1)| \tag{40}$$

$$\breve{\gamma} = \gamma\max_{\nu_1\in[0,1]}|Q(\nu_1)| \tag{41}$$

Due to the fact that $\nu_1(T) = 0$, this inequality establishes that the closed-loop system (7) with (21) is FT-ISS+C. In order to obtain the uniform boundedness in t of the joint torques τ over the interval $[0, T)$, it is necessary to examine the structure of the controller (21). This control law is a function of the joint angles q, the joint velocities $\dot{q}$, the reference joint accelerations $\ddot{q}_r$, and the scaled state z. (38), it can be observed that Z, and therefore z and w are uniformly bounded in t. From (39), it is similarly observed that E, and therefore ε, and $\dot{\varepsilon}$ are uniformly bounded in t. From

Fig. 3 Baxter tracking a desired trajectory under the prescribed-time control scheme, correcting for a large initial tracking error of 20 degrees in each joint and attenuating a sinusoidal torque disturbance of $D(t) = 0.1\sin(5t)$. The circles represent the reference trajectory to be tracked, and are spaced at approximately 1 s intervals.

Assumption 3, the uniform boundedness in t of q_r, $\dot{q}_r$, and $\ddot{q}_r$ are established. Furthermore, since ε, $\dot{\varepsilon}$, q_r, and $\dot{q}_r$ are uniformly bounded in t, q and $\dot{q}$ must also be uniformly bounded in t. Applying the uniform boundedness in t of each of these terms to (21), the uniform boundedness in t of the input τ is established.

5 Remarks on Prescribed-Time Control Law

Through the substitution of the scaling transform (14) to the control law (21), it is possible to obtain an expression for the control law in terms of the joint angular position and velocity errors $\varepsilon, \dot{\varepsilon}$ rather than the scaled state z

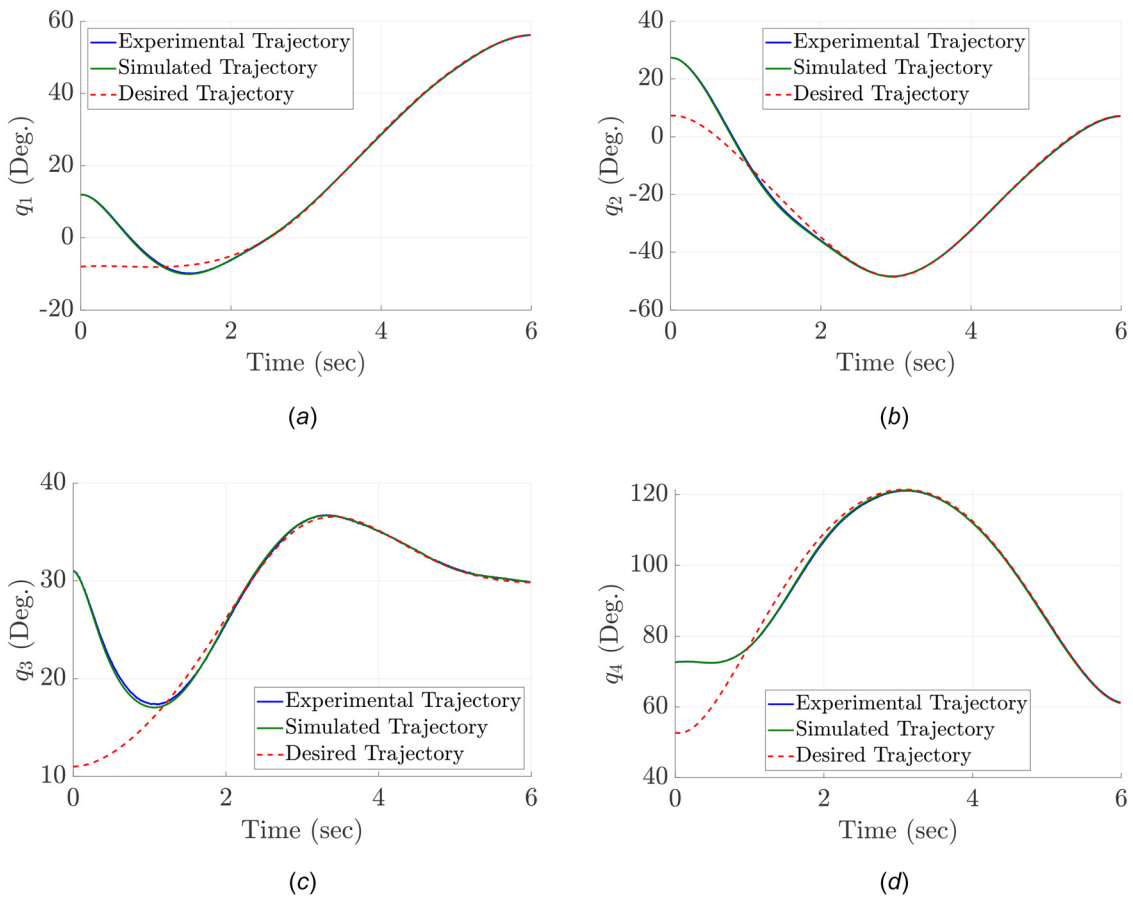

Fig. 4 The experimental, simulated, and desired joint trajectories of Baxter

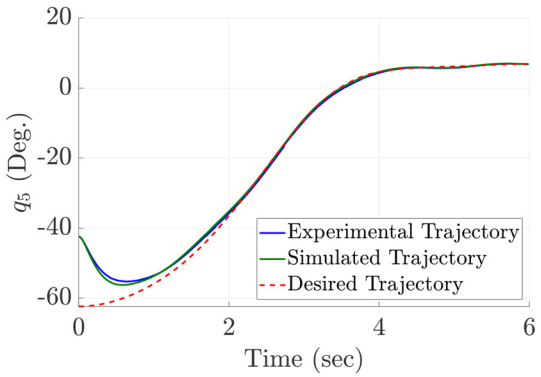

(e)

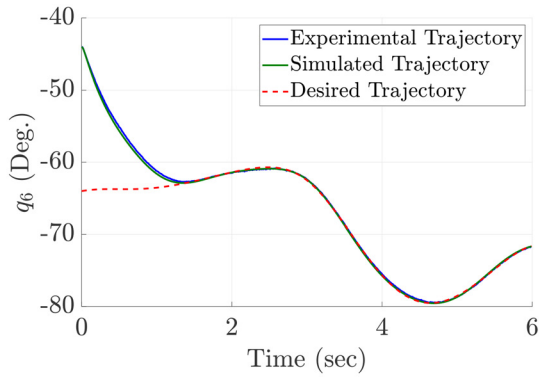

(f)

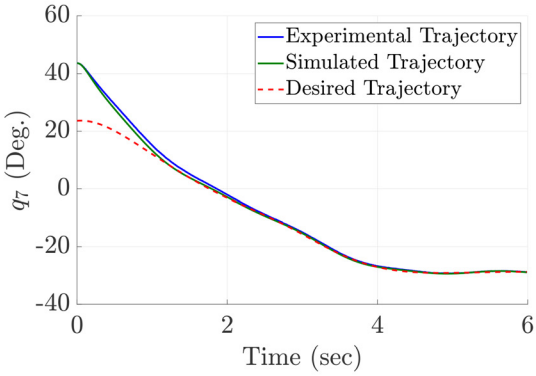

(g)

Fig. 4 (Continued)

$$\tau = -\mu_1^2 \hat{M}\left[\left(k+\theta+\eta\psi^2\right)\left(\left(\alpha+\mu_1\frac{2}{T}\right)\varepsilon+\dot{\varepsilon}\right)+\ddot{q}_r\right] + \hat{G}+\hat{F} \tag{42}$$

From this representation, the role of the controller parameters k, θ, η, and α can be observed. The sum $k+\theta$ is a scaled PD gain, and thus is the primary driver of the error signal to zero, η is the gain of the nonlinear damping term ψ, which aims to attenuate the effects of uncertainties on the control law, and α is a weighting factor which determines the ratio between the proportional and derivative gains of the control law. Thus, implementing the proposed prescribed-time control law control law requires the tuning of just three parameters (treating $k+\theta$ as one parameter), whose effect on the control law is readily observed. Furthermore, due to the direct dependence of the control law on the prescribed final time T, these three controller parameters need only be determined once for a given robot manipulator, regardless of the specific tasks the manipulator needs to perform. Thus, the proposed control law can be readily applied to a wide variety of tasks with different convergence time constraints.

A potential barrier to the practical application of this proposed method is the consequences of employing an unbounded gain $\mu_1(t)$. While the proposed control law guarantees boundedness of the control torques $\tau(t)$ even in the presence of nonvanishing uncertainties, problems may still arise due to measurement noise, numerical issues when multiplying large gains with small errors, and a finite controller frequency. In order to combat these practical issues, one effective strategy that can be employed is gain clipping. Using this strategy, we define the constants

$$\zeta = 1 - \bar{\mu}_1^{-1} = \frac{1-\bar{\mu}_1}{\bar{\mu}_1} \in (0,1) \tag{43}$$

$$\bar{\mu}_1^{-1} = \frac{1}{\bar{\mu}_1} = 1-\zeta \in (0,1) \tag{44}$$

$$\bar{\mu}_1 = \frac{1}{\bar{\mu}_1^{-1}} = \frac{1}{1-\zeta} \in (1,+\infty) \tag{45}$$

and redefine $\mu_1(t)$ in (42) as

$$\begin{aligned}\mu_1(t) &= \min\{\mu_1(t), \bar{\mu}_1\} \\ &= \frac{1}{\max\{\nu_1(t), \underline{\nu}_1(t)\}} \\ &= \frac{T}{T-\min\{t, \zeta T\}}\end{aligned} \tag{46}$$

This redefinition of (9) upper bounds the scaling gain μ_1 by the value $\bar{\mu}_1 = \frac{1}{1-\zeta}$, ensuring that the controller gains do not grow past the point where the previously mentioned issues begin to noticeably affect the closed-loop system. A consequence of this modification is that the regulation of the tracking errors is to a small neighborhood of zero, rather than exactly zero as when utilizing an unbounded gain. Employing a ζ that is sufficiently close to 1 can ensure that this neighborhood is negligible, achieving performance that is qualitatively similar to that of utilizing an unbounded gain.

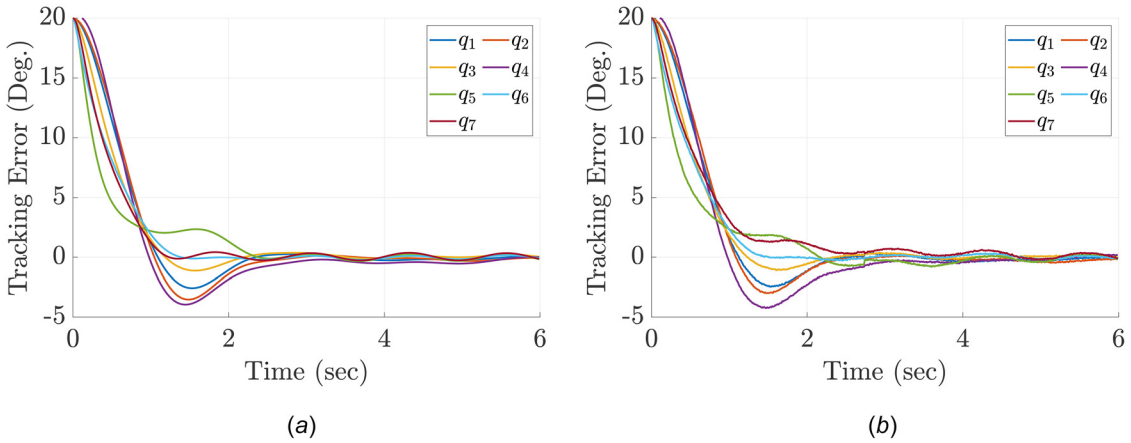

Fig. 5 The simulated (*a*) and experimental (*b*) joint tracking errors of Baxter, with $D(t) = 0{:}1\sin(5t)$

6 Simulation and Experimental Results

In order to assess the performance of the proposed prescribed-time approach, we perform both a simulation using ODE methods on Baxter's dynamic Eq. (1), as well as an experiment. In both the simulation and experiment, Baxter must track a trajectory designed for a pick and place task in Ref. [33], while under the influence of a torque disturbance of $D(t) = 0.1\sin(5t)$ applied to each joint. In addition, this task is purposely started from a large initial angular position error of 20 deg for each joint. Thus, this simulation and experiment demonstrate the ability of the proposed method to converge from a large initial condition to the desired trajectory within the prescribed finite time, while rejecting a large torque disturbance. The controller parameters used in both the simulation and experiment are $T = 6$, $k + \theta = 5$, $\eta = 0.005$, $\alpha = 2$, and $\zeta = 0.4$. Note that $\bar{\mu}_1^2$, which is employed in lieu of μ_1^2 in (42), which would without clipping go to infinity, is as low as 2.78.

From Fig. 3 it can be observed that the prescribed-time controller is successful at executing the pick-and-place task in practice. Comparing the reference trajectory, highlighted by the green circles in the figure, to the initial position of Baxter's right end effector located at the bottom of the figure, it can be seen that an angular position error of 20 deg in each joint corresponds to a large error in Cartesian coordinates. Despite this large initial tracking error, the prescribed-time controller is shown to be effective at quickly attenuating this tracking error, and achieving close

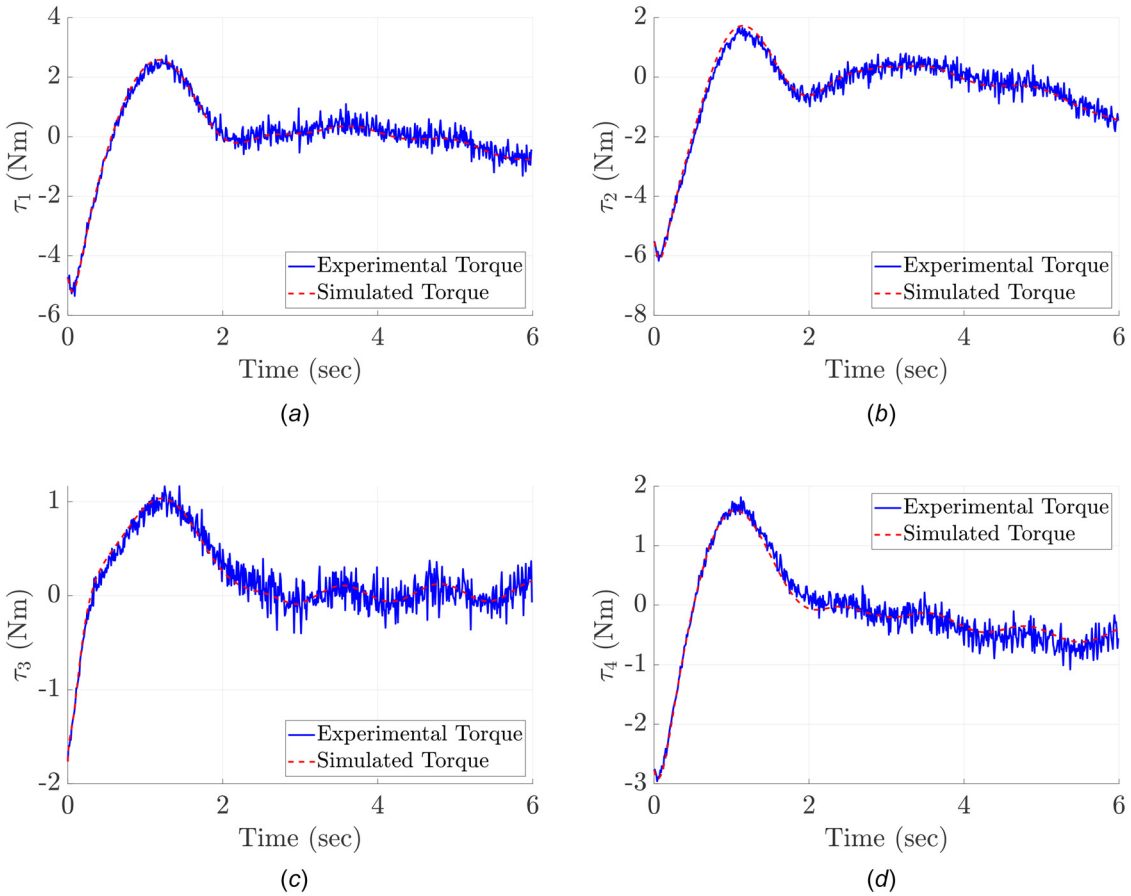

Fig. 6 The experimental and simulated joint torque input signals of Baxter

tracking of the desired trajectory for the remainder of the operation. After only 1 s of operation, the distance between the desired trajectory and Baxter's right end effector is significantly reduced, and after 3 s of operation, Baxter's right end effector appears to coincide exactly with the desired trajectory.

The experimental, simulated and desired joint trajectories can be seen in Fig. 4. Despite the large initial joint tracking errors, as well as the large sinusoidal disturbance applied to the system, negligible tracking errors are achieved after around 2.5 s of operation. Throughout the procedure, oscillations in the joint angular positions cannot be observed from this figure, indicating that the nonlinear-damping method employed was effective at absorbing the effect of the sinusoidal disturbance. Furthermore, minimal overshoot is observed during the 1st 2.5 s of operation, indicating that the proposed control law is acting neither too aggressively or too leniently in the beginning of the task. Observing Fig. 5, it is possible to see the convergence behavior of the proposed method in more detail. After 2.5 s of operation, roughly coinciding with the time of $\zeta T = 2.4$ seconds where the gain multiplier μ_1 stops increasing, the majority of the tracking errors have already been significantly attenuated. From 2.5 s onward, the residual tracking errors, mostly resulting from the sinusoidal torque disturbance, are attenuated to an acceptably small value of less than 0.2 deg.

The experimental and simulated joint toque input signals can be seen in Fig. 6. It is important to note that these torques are significantly lower than the maximum torque output of Baxter's joints, which are 50 Nm for joints 1–4, and 15 Nm for joints 5–7. Thus, the prescribed-time approach is able to correct for a large initial error without producing excessive joint torques. Additionally, the simulated torques remain smooth throughout the procedure and do not display chattering, which can negatively affect the lifespan of the actuators used to control the robot manipulator. Furthermore, while the presence of noise in angular velocity measurements has caused similar variations in the experimental joint torques, these torques still exhibit moderate continuity and do not appear to be affected by chattering. An important observation regarding both the simulated and experimental joint torques is that oscillation can be observed throughout the procedure, which is most noticeable in joint 7. Both the peak-to-peak difference in this observed oscillation, as well as its frequency closely match that of the applied torque disturbance $D(t) = 0.1\sin(5t)$, indicating that the proposed controller is able to" absorb" the disturbance as the prescribed final time of 6 s is reached.

In order to verify the ability of the proposed method to reject a torque disturbance with a nonzero mean, an additional simulation and experiment were performed with a torque disturbance of $D(t) = 0.1\sin(5t) + 0.05$. In the interest of brevity, we present only the convergence of the joint tracking errors, which can be seen in Fig. 7. It can be observed from this figure that both the simulated and experimental tracking errors display nearly identical behavior to Fig. 6, demonstrating that the convergence of the proposed method is not negatively effected by a disturbance torque with a nonzero mean.

7 Conclusion

In this research effort, we formulated and experimentally verified the prescribed-time trajectory tracking control of a 7-DOF robot manipulator. In order to ensure regulation of the tracking errors by the prescribed final time, we employed a scaling of the state by a function of time that grows unbounded toward the terminal time. Through Lyapunov analysis, we demonstrated that the proposed controller achieves regulation of all tracking errors within the prescribed time with a torque that is uniformly bounded, even in the presence of a matched nonvanishing disturbance. Through inspection of the control law, we demonstrated that the choice of parameters for the proposed control law is intuitive

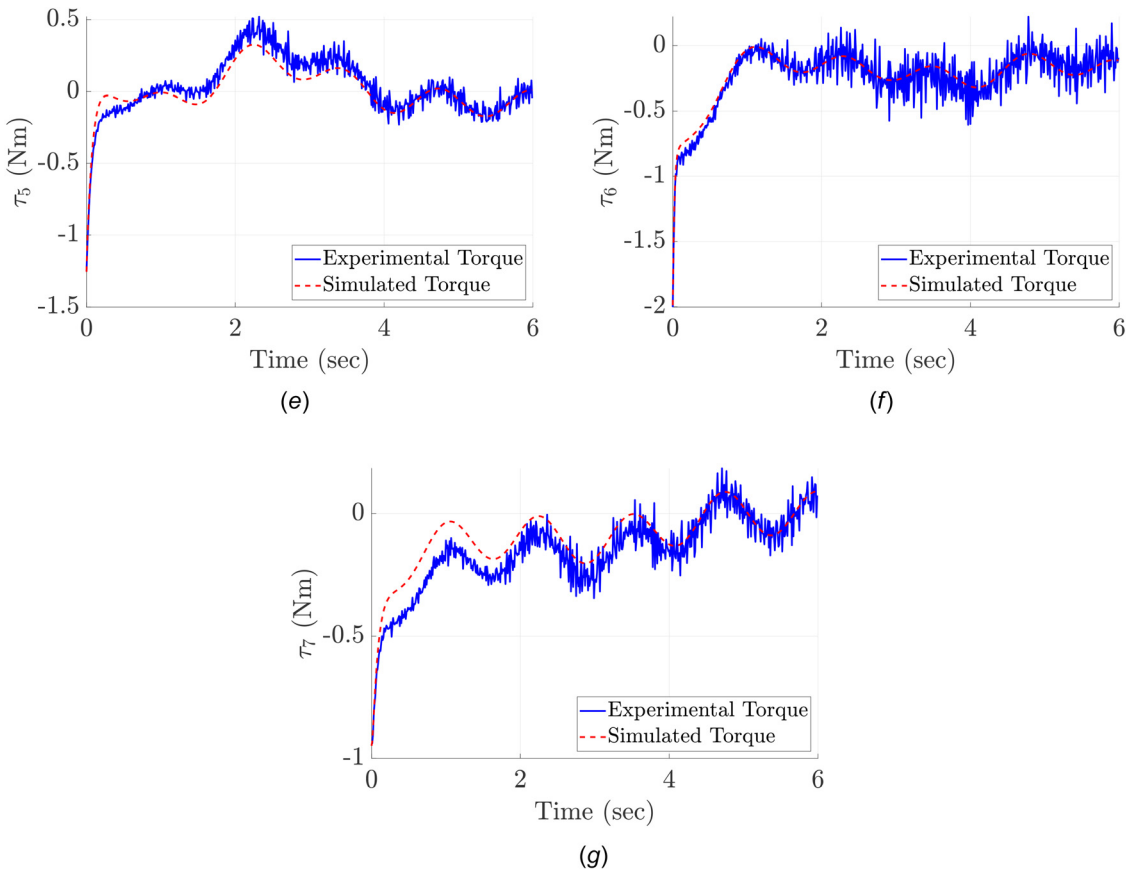

Fig. 6 (Continued)

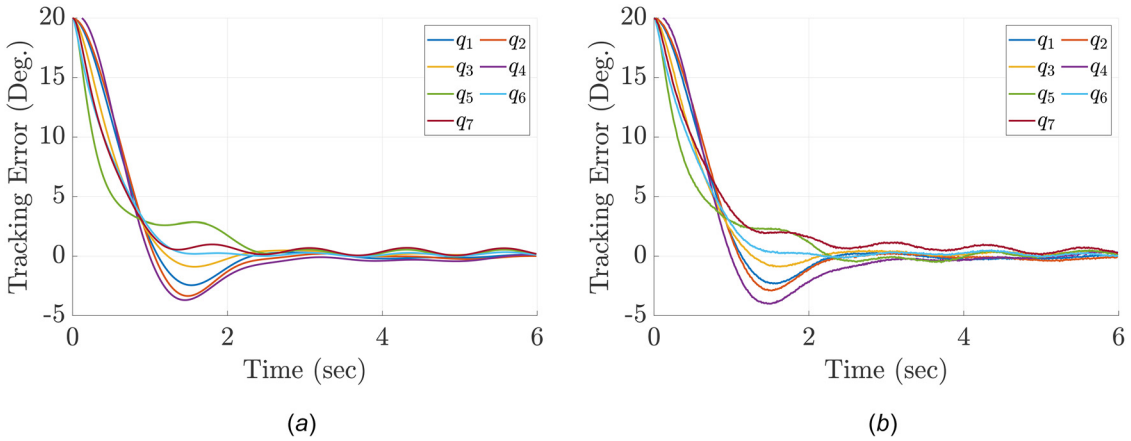

Fig. 7 The simulated (*a*) and experimental (*b*) joint tracking errors of Baxter, when subjected to a disturbance with nonzero mean $D(t) = 0.1\sin(5t) + 0.05$

and straightforward, and that the controller could be implemented in a practical system with minimal modifications. Then, through both simulation and experiment, we demonstrated that the proposed controller is capable of converging to the desired trajectory within the prescribed time, despite large initial conditions of the tracking errors and a sinusoidal disturbance being applied in each joint.

Acknowledgment

This article is based upon work supported by the National Science Foundation under Award #1823951-1823983. The views and opinions of authors expressed herein do not necessarily state or reflect those of the United States Government or any agency thereof.

Funding Data

- National Science Foundation (Funder ID: 10.13039/100000001).

References

[1] Han, S. I., and Lee, J., 2016, "Finite-Time Sliding Surface Constrained Control for a Robot Manipulator With an Unknown Deadzone and Disturbance," ISA Trans., **65**, pp. 307–318.
[2] Hong, Y., Xu, Y., and Huang, J., 2002, "Finite-Time Control for Robot Manipulators," Syst. Control Letters, **46**(4), pp. 243–253.
[3] Yu, S., Yu, X., Shirinzadeh, B., and Man, Z., 2005, "Continuous Finite-Time Control for Robotic Manipulators With Terminal Sliding Mode," Automatica, **41**(11), pp. 1957–1964.
[4] Yang, C., Jiang, Y., He, W., Na, J., Li, Z., and Xu, B., 2018, "Adaptive Parameter Estimation and Control Design for Robot Manipulators With Finite-Time Convergence," IEEE Trans. Ind. Electron., **65**(10), pp. 8112–8123.
[5] Zhao, D., Li, S., Zhu, Q., and Gao, F., 2010, "Robust Finite-Time Control Approach for Robotic Manipulators," IET Control Theory Appl., **4**(1), pp. 1–15.
[6] Wang, Y., Chen, M., and Song, Y., 2021, "Robust Fixed-Time Inverse Dynamic Control for Uncertain Robot Manipulator System," Complexity, **2021**, pp. 1–12.
[7] Zhang, D., Kong, L., Zhang, S., Li, Q., and Fu, Q., 2020, "Neural Networks-Based Fixed-Time Control for a Robot With Uncertainties and Input Deadzone," Neurocomputing, **390**, pp. 139–147.
[8] Su, Y., Zheng, C., and Mercorelli, P., 2020, "Robust Approximate Fixed-Time Tracking Control for Uncertain Robot Manipulators," Mech. Syst. Signal Process, **135**, p. 106379.
[9] Jin, X., 2019, "Adaptive Fixed-Time Control for MIMO Nonlinear Systems With Asymmetric Output Constraints Using Universal Barrier Functions," IEEE Trans. Autom. Control, **64**(7), pp. 3046–3053.
[10] Zhang, L., Wang, Y., Hou, Y., and Li, H., 2019, "Fixed-Time Sliding Mode Control for Uncertain Robot Manipulators," IEEE Access, **7**, pp. 149750–149763.
[11] Espitia, N., Polyakov, A., Efimov, D., and Perruquetti, W., 2019, "Boundary Time-Varying Feedbacks for Fixed-Time Stabilization of Constant-Parameter Reaction–Diffusion Systems," Automatica, **103**, pp. 398–407.
[12] Garg, K., and Panagou, D., 2021, "Robust Control Barrier and Control Lyapunov Functions With Fixed-Time Convergence Guarantees," 2021 American Control Conference (ACC), New Orleans, LA, May 25–28, pp. 2292–2297.
[13] Song, Y., Wang, Y., Holloway, J., and Krstic, M., 2017, "Time-Varying Feedback for Regulation of Normal-Form Nonlinear Systems in Prescribed Finite Time," Automatica, **83**, pp. 243–251.
[14] Song, Y., Wang, Y., and Krstic, M., 2019, "Time-Varying Feedback for Stabilization in Prescribed Finite Time," Int. J. Robust Nonlinear Control, **29**(3), pp. 618–633.
[15] Becerra, H. M., Vázquez, C. R., Arechavaleta, G., and Delfin, J., 2018, "Predefined-Time Convergence Control for High-Order Integrator Systems Using Time Base Generators," IEEE Trans. Control Syst. Technol., **26**(5), pp. 1866–1873.
[16] Obregon-Flores, J., Arechavaleta, G., Becerra, H. M., and Morales-Diaz, A., 2021, "Predefined-Time Robust Hierarchical Inverse Dynamics on Torque-Controlled Redundant Manipulators," IEEE Trans. Rob., **37**(3), pp. 962–978.
[17] Muñoz-Vázquez, A. J., Sánchez-Torres, J. D., Jimenez-Rodriguez, E., and Loukianov, A. G., 2019, "Predefined-Time Robust Stabilization of Robotic Manipulators," IEEE/ASME Trans. Mechatronics, **24**(3), pp. 1033–1040.
[18] Sánchez-Torres, J. D., Muñoz-Vázquez, A. J., Defoort, M., Jiménez-Rodríguez, E., and Loukianov, A. G., 2020, "A Class of Predefined-Time Controllers for Uncertain Second-Order Systems," Eur. J. Control, **53**, pp. 52–58.
[19] Cao, Y., and Song, Y.-D., 2020, "Adaptive PID-Like Fault-Tolerant Control for Robot Manipulators With Given Performance Specifications," Int. J. Control, **93**(3), pp. 377–386.
[20] Cao, Y., Cao, J., and Song, Y., 2021, "Practical Prescribed Time Control of Euler-Lagrange Systems With Partial/Full State Constraints: A Settling Time Regulator-Based Approach," IEEE Trans. Cybern., pp. 1–10.
[21] Krishnamurthy, P., Khorrami, F., and Krstic, M., 2021, "Adaptive Output-Feedback Stabilization in Prescribed Time for Nonlinear Systems With Unknown Parameters Coupled With Unmeasured States," Int. J. Adaptive Control Signal Process, **35**(2), pp. 184–202.
[22] Li, W., and Krstic, M., 2022, "Stochastic Nonlinear Prescribed-Time Stabilization and Inverse Optimality," IEEE Trans. Autom. Control, **67**(3), pp. 1179–1193.
[23] Steeves, D., Krstic, M., and Vazquez, R., 2020, "Prescribed–Time Estimation and Output Regulation of the Linearized Schrödinger Equation by Backstepping," Eur. J. Control, **55**, pp. 3–13.
[24] Holloway, J., and Krstic, M., 2019, "Prescribed-Time Observers for Linear Systems in Observer Canonical Form," IEEE Trans. Autom. Control, **64**(9), pp. 3905–3912.
[25] Krishnamurthy, P., Khorrami, F., and Krstic, M., 2020, "A Dynamic High-Gain Design for Prescribed-Time Regulation of Nonlinear Systems," Automatica, **115**, p. 108860.
[26] Khalil, H. K., and Grizzle, J. W., 2002, *Nonlinear Systems*, **3**, Prentice Hall, Upper Saddle River, NJ.
[27] Bagheri, M., and Naseradinmousavi, P., 2017, "Novel Analytical and Experimental Trajectory Optimization of a 7-DOF Baxter Robot: Global Design Sensitivity and Step Size Analyses," Int. J. Adv. Manuf. Technol., **93**(9–12), pp. 4153–4167.
[28] Bagheri, M., Naseradinmousavi, P., and Morsi, R., 2017, "Experimental and Novel Analytical Trajectory Optimization of a 7-DOF Baxter Robot: Global Design Sensitivity and Step Size Analyses," ASME Paper No. DSCC2017-5004.
[29] Bagheri, M., Krstić, M., and Naseradinmousavi, P., 2018, "Joint-Space Trajectory Optimization of a 7-DOF Baxter Using Multivariable Extremum Seeking," 2018 Annual American Control Conference (ACC), Milwaukee, WI, June 27–29, pp. 2176–2181.
[30] Bagheri, M., Krstić, M., and Naseradinmousavi, P., 2018, "Multivariable Extremum Seeking for Joint-Space Trajectory Optimization of a High-Degrees-of-Freedom Robot," ASME J. Dyn. Syst. Meas. Control, **140**(11), p. 111017.
[31] Bagheri, M., Krstić, M., and Naseradinmousavi, P., 2018, "Analytical and Experimental Predictor-Based Time Delay Control of Baxter Robot," ASME Paper No. DSCC2018-9101.

[32] Bagheri, M., Naseradinmousavi, P., and Krstić, M., 2019, "Feedback Linearization Based Predictor for Time Delay Control of a high-DOF Robot Manipulator," Automatica, **108**, p. 108485.
[33] Bertino, A., Bagheri, M., Krstić, M., and Naseradinmousavi, P., 2019, "Experimental Autonomous Deep Learning-Based 3D Path Planning for a 7-DOF Robot Manipulator," ASME Paper No. DSCC2019-8951.
[34] Bagheri, M., Naseradinmousavi, P., and Krstić, M., 2019, "Time Delay Control of a High-DOF Robot Manipulator Through Feedback Linearization Based Predictor," ASME Paper No. DSCC2019-8915.
[35] Bertino, A., Naseradinmousavi, P., and Kelkar, A., 2021, "Analytical and Experimental Decentralized Adaptive Control of a High-Degrees-of-Freedom Robot Manipulator," ASME J. Dyn. Syst. Meas. Control, **143**(7), p. 071007.
[36] Bertino, A., Naseradinmousavi, P., and Krstic, M., 2021, "Experimental and Analytical Delay-Adaptive Control of a 7-DOF Robot Manipulator," 2021 American Control Conference (ACC), New Orleans, LA, May 25–28, pp. 72–77.
[37] Bertino, A., Naseradinmousavi, P., and Kelkar, A., 2020, "Experimental and Analytical Decentralized Adaptive Control of a 7-DOF Robot Manipulator," ASME Paper No. DSCC2020-3181.
[38] Bertino, A., Naseradinmousavi, P., and Krstić, M., 2022, "Delay-Adaptive Control of a 7-DOF Robot Manipulator: Design and Experiments," IEEE Trans. Control Syst. Technol., pp. 1–16.